mathematics

Article

Chaotic Dynamics of Non-Autonomous Nonlinear System for a Sandwich Plate with Truss Core

Dongmei Zhang and Feng Li *

School of Mathematics and Statistics, Linyi University, Linyi 276005, China; zhangdongmei@lyu.edu.cn
* Correspondence: lifeng@lyu.edu.cn; Tel.: +86-135-1869-5076

Abstract: This paper deals with the multi-pulse chaotic dynamics of a sandwich plate with truss core under transverse and in-plane excitations. In order to analyze the complicated nonlinear behaviors of the sandwich plate model by means of the improved extended Melnikov technique, the two-degrees non-autonomous system is transformed into an appropriate form. Through theoretical analysis, the sufficient conditions for the existence of multi-pulse homoclinic orbits and the criterion for the occurrence of chaotic motion are obtained. The damping coefficients and transverse excitation parameters are considered as the control parameters to discuss chaotic behaviors of the sandwich plate system. Numerical results and the maximal Lyapunov exponents are performed to further test the existence of the multi-pulse jumping orbits. The theoretical predictions and numerical results demonstrate that the chaos phenomena may exist in the parametrical excited sandwich plate.

Keywords: chaos; multi-pulse orbit; extended Melnikov method; Lyapunov exponent

MSC: 37G25

Citation: Zhang, D.; Li, F. Chaotic Dynamics of Non-Autonomous Nonlinear System for a Sandwich Plate with Truss Core. *Mathematics* **2022**, *10*, 1889. https://doi.org/10.3390/math10111889

Academic Editors: Zhouchao Wei and Liguo Yuan

Received: 25 April 2022
Accepted: 27 May 2022
Published: 31 May 2022

1. Introduction

The truss core sandwich materials belong to a new type of lightweight structure and are widely used in mechanical engineering and other various areas. Different types of sandwich structures have attracted the attention of many researchers. Analytical and numerical techniques can be applied to investigate the resonant response, bifurcation and chaotic dynamics for these sandwich materials.

For instance, Chen et al. [1,2] discussed the stability and nonlinear response of the harmonic-excited plate with tetrahedral core under influence of thermal loads. Boorle and Mallick [3] studied the global response of composite sandwich plates to the effect of some geometric parameters. In 2014, Zhang et al. [4] studied the periodic and chaotic motions of the sandwich plate with truss core. The influence of different excitation parameters on nonlinear dynamic behaviors were investigated by numerical methods. By introducing the nonlinear wave equation, Zhang et al. [5] applied the Menikov method to confirm the chaotic motions for this sandwich plate. Furthermore, based on the model given in [4], Chen et al. [6] discussed the local bifurcations and slow-fast motions for this four-dimensional nonlinear system under slow parametric and fast external excitation. However, the multi-pulse chaotic dynamics of this system have not been studied analytically. Based on the dimensionless governing equation, we conduct further research to obtain the conditions for the occurrence of chaotic motion by theoretical methods.

The bifurcation problems [7,8], single-pulse orbits and multi-pulse orbits [9] have been the top issue in dynamic research. Many researchers have developed analytical methods to study chaotic motions for the high-dimensional nonlinear systems. The Melnikov method is a classical approach to detect chaotic dynamics which was developed by Wiggins, Kovacic and Yagasaki. In 1998, Camassa et al. [10] proposed an extended Melnikov method which may be employed to deal with the multi-pulse jumping orbits for a class of Hamiltonian systems with perturbation. Subsequently, Yagasaki [11,12] developed the

Melnikov method to investigate the chaotic dynamics of high-dimensional non-autonomous systems. The paper [13] demonstrates how to employ the extended Melnikov method to analyze the multi-pulse chaotic dynamics for the parametrically excited viscoelastic moving belt. Afterwards, Zhang et al. [14] investigated the chaotic dynamics of the rotating ring truss antenna. The double parameter homoclinic orbits were detected by means of the extended Melnikov function. In [15], Zhang and Chen proved the existence of single-pulse jumping homoclinic orbits of the sandwich plate with truss core on a certain parameter range. Ahmadi et al. [16] investigated a new five-dimensional chaotic system. The phenomenon of extreme multi-stability are considered for the variety of conditions. In [17], many complex dynamic behaviors of another 5D chaotic system with equilibrium were discovered.

These analytical techniques can deal with autonomous systems. In most instances, we need to discuss the dynamical problems of non-autonomous systems. The literature [18] used the improved Melnikov method to detect the chaotic behaviors of the buckled thin plate model. In 2012, Zhang et al. [19] studied the chaotic dynamics of another type of sandwich plate. Based on the non-autonomous nonlinear governing equations, Wu et al. [20] investigated the global bifurcations for the circular mesh antenna model. It is worth mentioning that the Melnikov method is improved to handle six-dimensional nonlinear systems by Zhang and Hao in papers [21].

The paper handles the global bifurcation and chaotic motion of a simply supported sandwich plate with truss core subjected to parametrical excitations. From the explicit formulas of normal form, the improved extended Melnikov method [10,18] is used to study the chaotic dynamics for this non-autonomous system. The damping coefficients and transverse excitation parameters are chosen as the control parameters to discuss the influence on the dynamic behaviors of the sandwich plate system with truss core. The numerical results also show that the chaotic motions may occur for the sandwich plate with truss core subject to parametrical excitations which demonstrates the validation of the theoretical prediction.

The paper is outlined as follows. In Section 2, the main theory of the extended Melnikov method for the non-autonomous system is exhibited. In Section 3, the dynamical model is described for the sandwich plate with truss core under transverse and in-plane excitations. The chaotic motions of the four dimensional non-autonomous systems are analyzed based on the improved extended Melnikov method. In Section 4, based on the phase portraits, waveforms and Lyapunov exponents, numerical simulations are utilized to study the dynamic behaviors of the sandwich plate. Finally, we give the conclusions in Section 5.

2. Formulation

The main theory of the improved Melnikov method [10,18] for the non-automonous nonlinear system will be listed in this section. Consider a general Hamilton system:

$$\begin{aligned}
&\dot{x} = JD_xH(x, v_1) + \epsilon g^x(x, v, \phi, \mu, \epsilon),\\
&\dot{v_1} = \epsilon g^{v_1}(x, v, \phi, \mu, \epsilon),\\
&\dot{v_2} = \Omega(x, v_1) + \epsilon g^{v_2}(x, v, \phi, \mu, \epsilon),\\
&\dot{\phi} = \omega,
\end{aligned} \tag{1}$$

where $x = (x_1, x_2) \in R^2$, $0 < \epsilon << 1$, $\mu \in R^p$ represents the parameters in the perturbed system. D_x indicates the partial derivatives about x, $g = (g^x, g^{v_1}, g^{v_2})$ denotes a periodic function of t. When $\epsilon = 0$, the unperturbed system can be given by

$$\begin{aligned}
&\dot{x} = JD_xH(x, v_1),\\
&\dot{v_1} = 0,\\
&\dot{v_2} = \Omega(x, v_1),
\end{aligned} \tag{2}$$

which is an uncoupled nonlinear dynamical system. The following two assumptions are required according to the results of [10].

Assumption 1. *For every $v_1 \in [R_1, R_2]$, there exist a hyperbolic equilibrium $x = x_0(v_1)$ and a homoclinic orbit $x^h(t, v_1)$ connected to $x_0(v_1)$.*

Assumption 2. *For some $v_1 = v_{10} \in [R_1, R_2]$, the function Ω satisfies the following conditions*

$$\Omega(x_0(v_{10}), v_{10}) = 0, \frac{d\Omega(x_0(v_1), v_1)}{dv_1}(v_{10}) \neq 0.$$

From Assumption 2, we may find simple zeros about v_1 which can be called the resonance bands. A partial manifold is defined as

$$M = \{(x, v)|x = x_0(v_1), R_1 \leq v_1 \leq R_2, -L < v_2 < L\},$$

which is normally hyperbolic and possesses three-dimensional stable manifolds $W^s(M)$ and unstable manifolds $W^u(M)$. The existence of the homoclinic orbit of system (2) indicates that the stable manifolds $W^s(M)$ and unstable manifolds $W^u(M)$ intersect non-transversally along Γ, which can be given

$$\Gamma = \{(x, v)|x = x^h_{\pm}(t, v_1), R_1 \leq v_1 \leq R_2, v_2 = \int_{-\infty}^{t} D_{v_1} H(x^h, v_1) ds + v_{20}\}.$$

The perturbed system (1) is a five-dimensional system. In order to investigate the dynamics of non-autonomous systems, a cross-section is introduced in the phase space. The expression of cross section is defined as

$$\Sigma^{\phi_0} = \{(x, v_1, v_2, \phi)|\phi = \phi_0\}. \tag{3}$$

The variable ϕ is first fixed on Σ^{ϕ_0} and then vary throughout the circle S^1. In the full five-dimensional phase space $R^4 \times S^1$, the invariant manifold $M(t)$ can be written by

$$M(t) = \{(x, v, \phi)|x = x_0(v_1), R_1 \leq v_1 \leq R_2, -L < v_2 < L, \phi = \omega t + \phi_0\}. \tag{4}$$

Based on the analysis in [10], it can be known that $M(t)$ is a three-dimensional normally hyperbolic invariant manifold and the expression of the manifold $M_\epsilon(t)$ is written as

$$M_\epsilon(t) = \{(x, v, \phi)|x = x_0(v_1) + O(\epsilon), R_1 \leq v_1 \leq R_2, -L < v_2 < L, \phi = \omega t + \phi_0\}. \tag{5}$$

The manifolds $M_\epsilon(t)$, $W^s_\epsilon(M(t))$ and $W^u_\epsilon(M(t))$ are C^r ϵ-close to the manifolds $M(t)$, $W^s(M(t))$ and $W^u(M(t))$, respectively. The 1-pulse Melnikov function and k-pulse Melnikov function [10] in the Cartesian coordinate are shown by

$$\begin{aligned} M(v_0, \phi_0, \mu) &= \int_{-\infty}^{+\infty} \langle n(p^h(t)), g(p^h(t), \omega t + \phi_0, \mu, 0)\rangle dt, \\ M_k(v_0, \phi_0, \mu) &= \sum_{j=0}^{k-1} M(v_{10}, v_{20} + j\Delta v_2(v_{10}), \phi_0, \mu), \end{aligned} \tag{6}$$

where symbol$\langle , \rangle$ denotes the Euclidean inner product of two functions,

$$\begin{aligned} &n = (D_x H(x, v_1), (D_{v_1} H(x, v_1) - (D_{v_1} H(x(v_{10}), v_1), 0), \\ &g = (g^x(x, v, \omega t, \mu, 0), g^{v_1}(x, v, \omega t, \mu, 0), g^{v_2}(x, v, \omega t, \mu, 0)), \\ &p^h(t) = (x^h(t, v_1), v_1, v_2^h(t, v_1) + v_{20}). \end{aligned} \tag{7}$$

and

$$\Delta v_2(v_{10}) = \int_{-\infty}^{+\infty} \Omega(x^h(\tau, v_1), v_{10}) d\tau. \tag{8}$$

The term Δv_2 denotes the distance between two equilibrium points. From Assumption 2, we may find that the vector x is located on a fast manifold. No manifold is on the manifold M. This means the nonfolding condition in [10] is satisfied naturally. Thus, there exist some integer k, $v_{20} = \bar{v}_{20}$, $\phi = \bar{\phi}_0$, and $\mu = \bar{\mu}$, so that the k-pulse Melnikov function $M_k(v_0, \phi_0, \mu)$ has a simple zero point, namely

$$M_k(v_{10}, \bar{v}_{20}, \bar{\phi}_0, \bar{\mu}) = 0, D_{v_2} M_k(v_{10}, \bar{v}_{20}, \bar{\phi}_0, \bar{\mu}) \neq 0. \tag{9}$$

The stable manifold $W^s(M_\epsilon^{\phi_0})$ and unstable manifold $W^u(M_\epsilon^{\phi_0})$ intersect transversely along surface $\Sigma(\bar{v}_{20})$. This means that the perturbed system has multi-pulse homoclinic orbits.

3. Chaotic Analysis of Perturbed System

The model of the sandwich plate with truss core considered in this paper is exhibited in Figure 1 [4]. A Cartesian coordinate oxy system is established in the middle surface of the sandwich plate. It can be supposed that the displacements of a point in the middle surface are represented by u, v and w in the x, y and z directions, respectively. Moreover, a, b and h denote the length, width and thickness of the sandwich plate, respectively. The transverse excitation of the sandwich plate is denoted by $f = F(x, y)\cos\Omega_1 t$ and the in-plane excitation is represented by $p = p_0 - p_1 \cos\Omega_2 t$.

According to [4], the nonlinear partial differential equations of the sandwich plate are given as follows

$$\begin{aligned}
&\frac{\partial^2 u_0}{\partial x^2} + a_1 \frac{\partial w_0}{\partial x}\frac{\partial^2 w_0}{\partial x^2} + a_2 \frac{\partial w_0}{\partial y}\frac{\partial^2 w_0}{\partial x \partial y} + a_3 \frac{\partial^2 v_0}{\partial x \partial y} + a_4 \frac{\partial^2 w_0}{\partial y^2} + a_5 \frac{\partial w_0}{\partial x}\frac{\partial^2 w_0}{\partial y^2} \\
&= a_6 \ddot{u}_0 + a_7 \ddot{\varphi}_x + a_8 \frac{\partial \ddot{w}_0}{\partial x}, \\
&\frac{\partial^2 v_0}{\partial y^2} + b_1 \frac{\partial w_0}{\partial x}\frac{\partial^2 w_0}{\partial x^2} + b_2 \frac{\partial w_0}{\partial x}\frac{\partial^2 w_0}{\partial x \partial y} + b_3 \frac{\partial^2 u_0}{\partial x \partial y} + b_4 \frac{\partial^2 v_0}{\partial y^2} + a_5 \frac{\partial w_0}{\partial x}\frac{\partial^2 w_0}{\partial x^2} \\
&= b_6 \ddot{v}_0 + b_7 \ddot{\varphi}_y + b_8 \frac{\partial \ddot{w}_0}{\partial y}, \\
&\frac{\partial^2 w_0}{\partial x^2} + c_1 \frac{\partial w_0}{\partial x}\frac{\partial^2 u_0}{\partial x^2} + c_2 (\frac{\partial w_0}{\partial x})^2 \frac{\partial^2 w_0}{\partial x^2} + c_3 \frac{\partial w_0}{\partial x}\frac{\partial^2 v_0}{\partial x \partial y} + c_4 \frac{\partial w_0}{\partial x}\frac{\partial w_0}{\partial y}\frac{\partial^2 w_0}{\partial x \partial y} \\
&+ c_5 \frac{\partial u_0}{\partial x}\frac{\partial^2 w_0}{\partial x^2} + c_6 \frac{\partial v_0}{\partial y}\frac{\partial^2 w_0}{\partial x^2} + c_7 (\frac{\partial w_0}{\partial x})^2 \frac{\partial^2 w_0}{\partial y^2} + c_8 (\frac{\partial w_0}{\partial y})^2 \frac{\partial^2 w_0}{\partial x^2} \\
&+ c_9 \frac{\partial w_0}{\partial y}\frac{\partial^2 v_0}{\partial y^2} + c_{10} (\frac{\partial w_0}{\partial y})^2 \frac{\partial^2 w_0}{\partial y^2} + c_{11} \frac{\partial w_0}{\partial y}\frac{\partial^2 u_0}{\partial x \partial y} + c_{12} \frac{\partial u_0}{\partial y}\frac{\partial^2 w_0}{\partial y^2} + c_{13} \frac{\partial w_0}{\partial x}\frac{\partial^2 u_0}{\partial y^2} \\
&+ c_{14} \frac{\partial u_0}{\partial y}\frac{\partial^2 w_0}{\partial x \partial y} + c_{15} \frac{\partial u_0}{\partial x}\frac{\partial^2 w_0}{\partial y^2} + c_{16} \frac{\partial v_0}{\partial x}\frac{\partial^2 w_0}{\partial x \partial y} + c_{17} \frac{\partial w_0}{\partial y}\frac{\partial^2 v_0}{\partial x^2} + c_{18} \frac{\partial^3 \varphi_x}{\partial x^3} \\
&+ c_{19} \frac{\partial^3 \varphi_y}{\partial x^2 \partial y} + c_{20} \frac{\partial^4 w_0}{\partial x^4} + c_{21} \frac{\partial^4 w_0}{\partial y^4} + c_{22} \frac{\partial^3 \varphi_x}{\partial x \partial y^2} + c_{23} \frac{\partial^4 \varphi_x}{\partial x^2 \partial y^2} + c_{24} \frac{\partial^3 \varphi_y}{\partial y^3} + c_{25} \frac{\partial \varphi_y}{\partial y} \\
&+ c_{26} \frac{\partial^2 w_0}{\partial y^2} + c_{27} \frac{\partial \varphi_x}{\partial x} + c_{28} F \cos(\Omega_1 t) + c_{29} \gamma \dot{w}_0 + c_{30} (p_0 - p_1 \cos(\Omega_2 t)) \frac{\partial^2 w_0}{\partial x^2} \\
&= c_{31} \ddot{w}_0 + c_{32} \frac{\partial w_0}{\partial x^2} + c_{33} \frac{\partial w_0}{\partial 9^2} + c_{34} (\frac{\partial \ddot{u}_0}{\partial x} + \frac{\partial \ddot{v}_0}{\partial y}) + c_{35} (\frac{\partial \ddot{\varphi}_x}{\partial x} + \frac{\partial \ddot{\varphi}_y}{\partial y}), \\
&\frac{\partial^2 \varphi_x}{\partial x^2} + d_1 \frac{\partial^2 \varphi_y}{\partial x \partial y} + d_2 \frac{\partial^3 w_0}{\partial x^3} + d_3 \frac{\partial^3 w_0}{\partial x \partial y^2} + d_4 \frac{\partial^2 \varphi_x}{\partial y^2} + d_5 \varphi_x + d_6 \frac{\partial w_0}{\partial x} \\
&= d_7 \ddot{u}_0 + d_8 \ddot{\varphi}_x + d_9 \frac{\partial \ddot{w}_0}{\partial x}, \\
&\frac{\partial^2 \varphi_y}{\partial y^2} + e_1 \frac{\partial^2 \varphi_x}{\partial x \partial y} + e_2 \frac{\partial^3 w_0}{\partial y^3} + e_3 \frac{\partial^3 w_0}{\partial y \partial x^2} + e_4 \frac{\partial^2 \varphi_y}{\partial x^2} + e_5 \varphi_y + e_6 \frac{\partial w_0}{\partial y} \\
&= e_7 \ddot{v}_0 + e_8 \ddot{\varphi}_y + e_9 \frac{\partial \ddot{w}_0}{\partial y},
\end{aligned} \tag{10}$$

where

$$\begin{aligned} u &= u_0 + z\phi_x - z^3 \frac{4}{3h^2}(\phi_x + \frac{\partial w_0}{\partial x}), \\ v &= v_0 + z\phi_y - z^3 \frac{4}{3h^2}(\phi_y + \frac{\partial w_0}{\partial y}), \\ w &= w_0. \end{aligned} \tag{11}$$

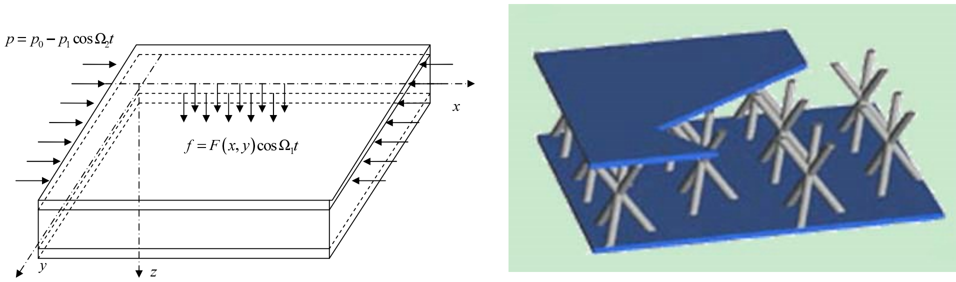

(**a**) (**b**)

Figure 1. The model of the sandwich plate with truss core: (**a**) schematic with the coordinate system; (**b**) the 3D-Kagome truss core sandwich structure.

Here, we mainly consider the first two modes of the sandwich plate. Applying the Galerkin technique, the two-degrees of freedom nonlinear equations of the sandwich plate with truss core were given as [4]

$$\begin{aligned} &\ddot{w}_1 + \mu_1 \dot{w}_1 + \beta_{11} w_1 + \beta_{16}(p_0 - p_1 \cos(\Omega_2 t)) w_1 + \beta_{12} w_1 w_2^2 + \beta_{13} w_2 w_1^2 + \beta_{14} w_1^3 \\ &\qquad + \beta_{15} w_2^3 = \beta_{17} F_1 \cos \Omega_1 t, \\ &\ddot{w}_2 + \mu_2 \dot{w}_2 + \beta_{21} w_2 + \beta_{26}(p_0 - p_1 \cos(\Omega_2 t)) w_2 + \beta_{22} w_2 w_1^2 + \beta_{23} w_1 w_2^2 + \beta_{24} w_2^3 \\ &\qquad + \beta_{25} w_1^3 = \beta_{27} F_2 \cos \Omega_1 t, \end{aligned} \tag{12}$$

where all the coefficients in (12) can be found in [4], w_1 and w_2 are the amplitudes of two modes, and Ω_1 and Ω_2 denote the frequencies of the transverse and in-plane excitations. Further, F_1 and F_2 represent the amplitudes of the transverse excitation corresponding to w_1 and w_2, respectively, and μ_1 and μ_2 are the damping coefficients.

Introducing the following transformations for Equation (12)

$$x_1 = w_1, x_2 = \dot{w}_1, x_3 = w_2, x_4 = \dot{w}_2,$$

this system can be given by

$$\begin{aligned} \dot{x_1} =& x_2, \\ \dot{x_2} =& -\beta_{11} x_1 - \beta_{12} x_1 x_3^2 - \beta_{13} x_3 x_1^2 - \beta_{14} x_1^3 - \beta_{15} x_3^3 - \mu_1 x_2 + F_1 \cos \Omega_1 t \\ & - f_1 x_1 \cos \Omega_2 t, \\ \dot{x_3} =& x_4, \\ \dot{x_4} =& -\beta_{21} x_3 - \beta_{22} x_1^2 x_3 - \beta_{23} x_1 x_3^2 - \beta_{24} x_3^3 - \beta_{25} x_1^3 - \mu_2 x_4 + F_2 \cos \Omega_1 t \\ & - f_2 x_3 \cos \Omega_2 t, \end{aligned} \tag{13}$$

where $\beta_{11} \rightarrow \beta_{11} + \beta_{16}p_0$, $\beta_{12} \rightarrow \beta_{21} + \beta_{26}p_0$, $F_1 \rightarrow \beta_{17}F_1$, $F_2 \rightarrow \beta_{27}F_2$, $f_1 \rightarrow \beta_{16}p_1$, $f_2 \rightarrow \beta_{26}p_1$. If μ, f_1, f_2, F_1 and F_2 are considered as perturbation parameters, the system (13) can rewritten as

$$\begin{aligned}
\dot{x_1} &= x_2, \\
\dot{x_2} &= -\beta_{11}x_1 - \beta_{12}x_1x_3^2 - \beta_{13}x_3x_1^2 - \beta_{14}x_1^3 - \beta_{15}x_3^3, \\
\dot{x_3} &= x_4, \\
\dot{x_4} &= -\beta_{21}x_3 - \beta_{22}x_1^2x_3 - \beta_{23}x_1x_3^2 - \beta_{24}x_3^3 - \beta_{25}x_1^3.
\end{aligned} \tag{14}$$

The Maple program is applied to obtain the normal form without the perturbation parameters up to 3-order, namely

$$\begin{aligned}
\dot{x_1} &= x_2, \\
\dot{x_2} &= -\frac{1}{2}\beta_{12}x_1(x_3^2 + x_4^2) - \beta_{14}x_1^3, \\
\dot{x_3} &= x_4 + \frac{1}{2}\beta_{22}x_1^2x_4 + \beta_{24}(x_3^2 + x_4^2), \\
\dot{x_4} &= -\beta_{21}x_3 - \beta_{24}(x_3^2 + x_4^2) - \frac{1}{2}\beta_{22}x_1^2x_3.
\end{aligned} \tag{15}$$

It can be seen that the four terms $\beta_{13}x_1^2x_3$, $\beta_{15}x_3^3$, $\beta_{23}x_3^2x_1$, $\beta_{25}x_1^3$ in (14) can only have influence on higher order terms. Thus, the damping coefficients, the forces coefficients and the aforementioned four terms are considered as perturbation terms which can be added small positive parameter ϵ. Then, we have

$$\begin{aligned}
\dot{x_1} =& x_2, \\
\dot{x_2} =& -\beta_{11}x_1 - \beta_{12}x_1x_3^2 - \beta_{14}x_1^3 - \epsilon\beta_{15}x_3^3 - \epsilon\beta_{13}x_3x_1^2 - \epsilon\mu_1x_2 + \epsilon F_1\cos\Omega_1 t \\
&- \epsilon f_1x_1\cos\Omega_2 t, \\
\dot{x_3} =& x_4, \\
\dot{x_4} =& -\beta_{21}x_3 - \beta_{22}x_1^2x_3 - \beta_{24}x_3^3 - \epsilon\beta_{23}x_1x_3^2 - \epsilon\beta_{25}x_1^3 - \epsilon\mu_2x_4 + \epsilon F_2\cos\Omega_1 t \\
&- \epsilon f_2x_3\cos\Omega_2 t.
\end{aligned} \tag{16}$$

The frequencies Ω_1 and Ω_2 satisfy the relations $Z_1\phi = \Omega_1 t$, $Z_2\phi = \Omega_2 t$, where Z_1 and Z_2 are non-negative integers. The transformations are introduced for Equation (16)

$$x_1 = \sqrt{\frac{\beta_{12}}{\bar{\beta}_{22}}}u_1, x_2 = \sqrt{\frac{\beta_{12}}{\bar{\beta}_{22}}}u_2, x_3 = v_1, x_4 = \mu_2 v_2$$

We may obtain the Hamilton form with the perturbation

$$\begin{aligned}
\dot{u_1} =& u_2, \\
\dot{u_2} =& -\beta_{11}u_1 - \beta_{12}u_1v_1^2 - \bar{\beta}_{14}u_1^3 - \epsilon\mu_1u_2 - \epsilon\bar{\beta}_{13}u_1^2v_1 - \epsilon\bar{\beta}_{15}v_1^3 + \epsilon\bar{F}_1\cos Z_1\phi \\
&- \epsilon f_1u_1\cos Z_2\phi, \\
\dot{v_1} =& -\epsilon\mu_2v_2, \\
\dot{v_2} =& -\bar{\beta}_{21}v_1 - \beta_{12}u_1^2v_1 - \bar{\beta}_{24}v_1^3 - \epsilon\mu_2v_2 - \epsilon\bar{\beta}_{23}u_1^2v_1 - \epsilon\bar{\beta}_{25}v_1^3 + \epsilon\bar{F}_2\cos Z_1\phi \\
&- \epsilon\bar{f}_2v_1\cos Z_2\phi, \\
\dot{\phi} =& 1,
\end{aligned} \tag{17}$$

where $\bar{\beta}_{14} = \beta_{14}\frac{\beta_{12}}{\bar{\beta}_{22}}$, $\bar{\beta}_{13} = \beta_{13}\sqrt{\frac{\beta_{12}}{\bar{\beta}_{22}}}$, $\bar{\beta}_{15} = \beta_{15}\sqrt{\frac{\beta_{12}}{\bar{\beta}_{22}}}$, $\bar{\beta}_{21} = \frac{\beta_{21}}{\mu_2}$, $\bar{\beta}_{22} = \frac{\beta_{22}}{\mu_2}$, $\bar{\beta}_{23} = \frac{\beta_{13}}{\mu_2}\sqrt{\frac{\beta_{12}}{\bar{\beta}_{22}}}$, $\bar{\beta}_{24} = \frac{\beta_{24}}{\mu_2}$, $\bar{F}_1 = F_1\sqrt{\frac{\bar{\beta}_{22}}{\beta_{12}}}$, $\bar{f}_2 = \frac{f_2}{\mu_2}$, $\bar{F}_2 = \frac{F_2}{\mu_2}$.

According to the previous theoretical results, a cross-section Σ^{ϕ_0} is introduced in the full five-dimensional phase space. When $\epsilon = 0$, the expression of the unperturbed system is

$$\begin{aligned} \dot{u_1} &= u_2, \\ \dot{u_2} &= -\beta_{11}u_1 - \beta_{12}u_1v_1^2 - \bar{\beta}_{14}u_1^3, \\ \dot{v_1} &= 0, \\ \dot{v_2} &= -\bar{\beta}_{21}v_1 - \beta_{12}u_1^2v_1 - \bar{\beta}_{24}v_1^3. \end{aligned} \tag{18}$$

The Hamiltonian of (18) can be given as

$$H = \frac{1}{2}u_2^2 + \frac{1}{2}\beta_{11}u_1^2 + \frac{1}{4}\beta_{12}u_1^2v_1^2 + \frac{1}{4}\bar{\beta}_{14}u_1^4 + \frac{1}{4}\bar{\beta}_{24}v_1^4 + \frac{1}{2} - \bar{\beta}_{21}v_1^2$$

It can be seen that the system (18) is an uncoupled system. Considering the first two equations of (18)

$$\begin{aligned} \dot{u_1} &= u_2, \\ \dot{u_2} &= -\beta_{11}u_1 - \beta_{12}u_1v_1^2 - \bar{\beta}_{14}u_1^3. \end{aligned} \tag{19}$$

The Hamiltonian is given as

$$H_0(u_1, u_2) = \frac{1}{2}u_2^2 + \frac{1}{2}Ru_1^2 + \frac{1}{4}\bar{\beta}_{14}u_1^4, \tag{20}$$

where $R = \beta_{11} + \beta_{12}v_1^2$.

Here, we consider the stability of the equilibrium solution within a certain range of parameters, that is $\beta_{12} < 0$, $\bar{\beta}_{14} > 0$, $R = \beta_{11} + \beta_{12}v_1^2 < 0$. Let $\bar{R} = -R$. According to the condition $\beta_{11} + \beta_{12}v_1^2 < 0$, the domain of v_1 is that $v_1 > \sqrt{\frac{2\beta_{11}}{-\beta_{12}}}$.

The system (19) has three trivial solutions. The singular point $(u_1, u_2) = (0, 0)$ is a saddle point. The singular points $(u_1, u_2) = (\pm\sqrt{\frac{\bar{R}}{\bar{\beta}_{14}}}, 0)$ are two centers. In this case, system (19) can exhibit the homoclinic bifurcations. We may obtain the expression of the homoclinic orbits

$$\begin{aligned} u_1(t) &= \pm\sqrt{\frac{2\bar{R}}{\bar{\beta}_{14}}}\,\mathrm{sech}\,\sqrt{\bar{R}}t, \\ u_2(t) &= \pm\bar{R}\sqrt{\frac{2}{\bar{\beta}_{14}}}\,\mathrm{sech}\,\sqrt{\bar{R}}t\tanh\sqrt{\bar{R}}t. \end{aligned} \tag{21}$$

According to system (18), the resonant value can be obtained as $v_{10} = \sqrt{\frac{\bar{\beta}_{21}}{-\bar{\beta}_{24}}}$. At the same time, the condition $\sqrt{\frac{\bar{\beta}_{21}}{-\bar{\beta}_{24}}} > \sqrt{\frac{2\beta_{11}}{-\beta_{12}}}$, namely $\bar{\beta}_{21}\beta_{12} < 2\bar{\beta}_{24}\beta_{11}$ need to be satisfied. Thus, the correlation coefficients of system (18) also need to satisfy $\bar{\beta}_{24} < 0$, $\beta_{12}\bar{\beta}_{21} < 2\beta_{11}\bar{\beta}_{24}$. Then the phase shift can be calculated as

$$\Delta v_2 = \int_{-\infty}^{+\infty}(-\bar{\beta}_{21}v_1 - \beta_{12}u_1^2v_1 - \bar{\beta}_{24}v_1^3)dt = -\frac{4\beta_{12}}{\bar{\beta}_{14}}\sqrt{\frac{\bar{\beta}_{21}}{\bar{\beta}_{24}}}\bar{R}. \tag{22}$$

In light of Equation (18), the 1-pulse Melnikov function can be calculated as

$$
\begin{aligned}
M &= \int_{-\infty}^{+\infty} \mu_2[\bar{\beta}_{13}u_1^2 v_1 + \bar{\beta}_{15}v_1^3 - \mu_1 u_2 + F_1\cos(\Omega_1 t + Z_1\phi_0) - \mu_1 f_1 \cos(\Omega_2 t + Z_2\phi_0)]dt \\
&\quad - \int_{-\infty}^{+\infty} \mu_2 v_2[-\bar{\beta}_{21}v_1 - \beta_{12}u_1^2 v_1 - \bar{\beta}_{24}v_1^3]dt \\
&= -\frac{4\mu_1 \bar{R}^{\frac{3}{2}}}{3\bar{\beta}_{14}} - \frac{\pi f_2 \Omega_2^2}{\bar{\beta}_{14}}\sin(Z_2\phi_0)\operatorname{csch}\frac{\pi\omega}{2\sqrt{\bar{R}}} - \pi\Omega_1 F_1\sqrt{\frac{2}{\bar{\beta}_{14}}}\sin(Z_1\phi_0)\operatorname{sech}\frac{\pi\Omega_1}{2\sqrt{\bar{R}}} - \mu_2\Delta v_2 v_{20}.
\end{aligned} \tag{23}
$$

Further, we can calculate the k-pulse Melnikov function

$$
\begin{aligned}
M_k = &-\frac{4\mu_1 \bar{R}^{\frac{3}{2}}}{3\bar{\beta}_{14}}k - k\frac{\pi f_2 \Omega_2^2}{\bar{\beta}_{14}}\sin(Z_2\phi_0)\operatorname{csch}\frac{\pi\omega}{2\sqrt{\bar{R}}} \\
&- k\pi\Omega_1 F_1\sqrt{\frac{2}{\bar{\beta}_{14}}}\sin(Z_1\phi_0)\operatorname{sech}\frac{\pi\Omega_1}{2\sqrt{\bar{R}}} - \mu_2\Delta v_2 v_{20}k - \frac{k(k-1)}{2}\mu_2\Delta v_2^2.
\end{aligned} \tag{24}
$$

For the k-pulse Melnikov function M_k has simple zeros, the relevant parameters should satisfy

$$
\begin{aligned}
&-\frac{4\mu_1 \bar{R}^{\frac{3}{2}}}{3\bar{\beta}_{14}} - \frac{\pi f_2 \Omega_2^2}{\bar{\beta}_{14}}\sin(Z_2\phi_0)\operatorname{csch}\frac{\pi\omega}{2\sqrt{\bar{R}}} - \pi\Omega_1 F_1\sqrt{\frac{2}{\bar{\beta}_{14}}}\sin(Z_1\phi_0)\operatorname{sech}\frac{\pi\Omega_1}{2\sqrt{\bar{R}}} \\
&- \mu_2\Delta v_2 v_{20} - \frac{(k-1)}{2}\mu_2\Delta v_2^2 = 0.
\end{aligned} \tag{25}
$$

Equation (25) can be reformulated as

$$
\begin{aligned}
k = &-\frac{8\mu_1 \bar{R}^{\frac{3}{2}}}{3\bar{\beta}_{14}\mu_2\Delta v_2^2} - \frac{2\pi f_2 \Omega_2^2}{\bar{\beta}_{14}\mu_2\Delta v_2^2}\sin(Z_2\phi_0)\operatorname{csch}\frac{\pi\omega}{2\sqrt{\bar{R}}} \\
&- \frac{2\pi\Omega_1 F_1}{\mu_2\Delta v_2^2}\sqrt{\frac{2}{\bar{\beta}_{14}}}\sin(Z_1\phi_0)\operatorname{sech}\frac{\pi\Omega_1}{2\sqrt{\bar{R}}} - \frac{2v_{20}}{\Delta v_2^2} + 1.
\end{aligned} \tag{26}
$$

Then, the suitable parameters are chosen to satisfy the following condition

$$
D_{v_{20}}M_k = -\mu_2\Delta v_2 k = \frac{4\beta_{12}\mu_2 k}{\bar{\beta}_{14}}\sqrt{\frac{\bar{\beta}_{21}}{\bar{\beta}_{24}}\bar{R}} \neq 0. \tag{27}
$$

At the same time, the following expression should be a non-negative integer by selecting suitable parameters in Equation (26).

$$
\begin{aligned}
N = &-\frac{8\mu_1 \bar{R}^{\frac{3}{2}}}{3\bar{\beta}_{14}\mu_2\Delta v_2^2} - \frac{2\pi f_2 \Omega_2^2}{\bar{\beta}_{14}\mu_2\Delta v_2^2}\sin(Z_2\phi_0)\operatorname{csch}\frac{\pi\omega}{2\sqrt{\bar{R}}} \\
&- \frac{2\pi\Omega_1 F_1}{\mu_2\Delta v_2^2}\sqrt{\frac{2}{\bar{\beta}_{14}}}\sin(Z_1\phi_0)\operatorname{sech}\frac{\pi\Omega_1}{2\sqrt{\bar{R}}} - \frac{2v_{20}}{\Delta v_2^2}.
\end{aligned} \tag{28}
$$

If the stable manifold $W^s(M_\epsilon^{\phi_0})$ and unstable manifold $W^u(M_\epsilon^{\phi_0})$ of system (17) intersect transversely, there exist chaotic motions for the sandwich plate with truss core under parametricaly excitations.

4. Numerical Simulations

In order to test the analytical predictions, we choose the original system (12) to perform numerical simulations. The Runge–Kutta algorithm through the software Matlab is utilized to explore the existence of chaotic motions in the sandwich plate. This part mainly discusses the influence of the damping coefficient and in-plane excitation on chaotic motions of the sandwich plate model. So μ_1 and f are selected as the controlling parameters to discover the law for the complicated behaviors.

Considering the conditions $\beta_{12} < 0$, $\beta_{14} > 0$, $\beta_{21} < 0$ and $\beta_{24} > 0$, the parameters of system (12) are chosen as follows: $\mu_1 = \mu_2 = \mu = 0.4$, $\beta_{11} = 27.8$, $\beta_{16}p_0 = 0.05$, $\beta_{12} = -0.1$, $\beta_{16}p_1 = 0.05$, $\beta_{13} = -1.5$, $\beta_{14} = 32$, $\beta_{15} = -0.51$, $\beta_{17}F_1 = 85.8$, $\beta_{21} = -1.08$, $\beta_{26}p_0 = 0.057$, $\beta_{25} = -5$, $\beta_{22} = -23.2$, $\beta_{26}p_1 = 0.057$, $\beta_{23} = -15.1$, $\beta_{24} = 31.6$, $f = \beta_{27}F_2 = 13.3$. Initial conditions are selected as $(w_1, \dot{w}_1, w_2, \dot{w}_2) = (0.02, 0.01, 0.04, 0.01)$. Figure 2 exhibits the phase portraits and waveforms in plane or space. Moreover, the maximal Lyapunov exponent of system (12) is $0.585523 > 0$. It can be shown that there exist chaotic motions for the nonlinear system. It is demonstrated again the existence of Shilnikov-type multi-pulse orbits in the sense of Smale horseshoes of the truss core sandwich plate.

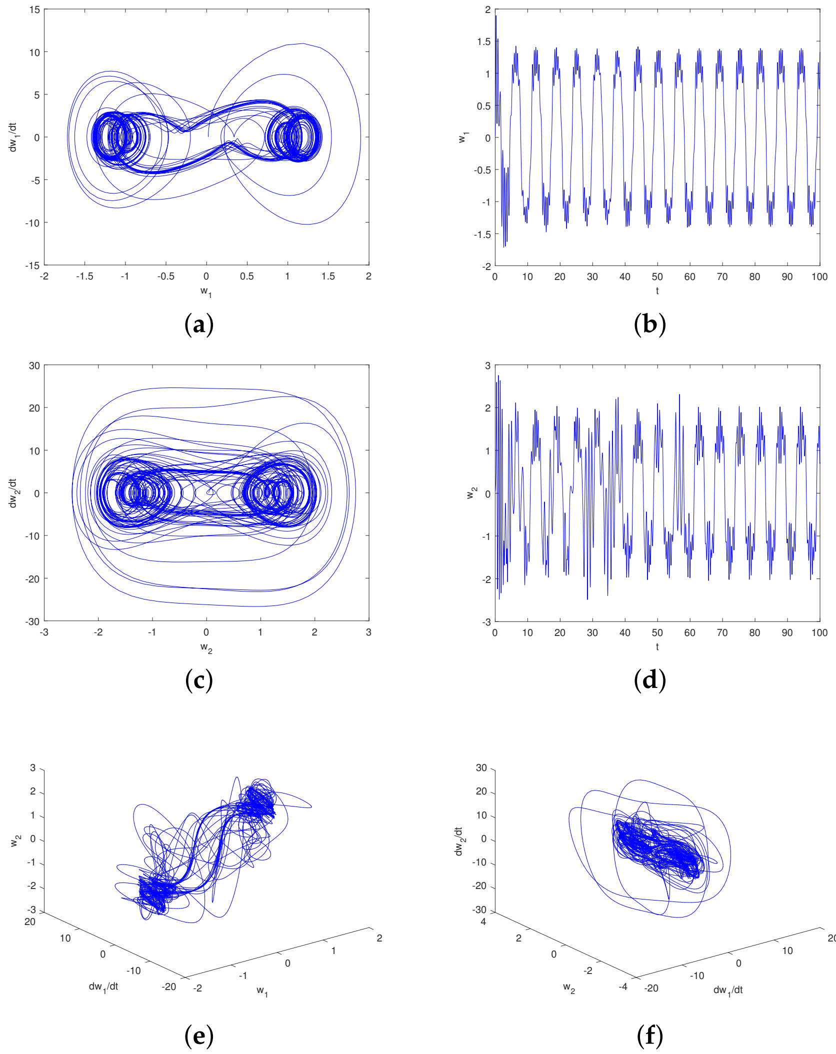

Figure 2. The phase portraits and waveforms of the sandwich plate with truss core when $\mu = 0.4$ and $f = 13.3$: (**a**) the phase portrait on plane $(w_1, \frac{dw_1}{dt})$; (**b**) the waveform on plane (t, w_1); (**c**) the phase portrait on plane $(w_2, \frac{dw_2}{dt})$; (**d**) the waveform on plane (t, w_2); (**e**) the phase portraits in the three-dimensional space $(w_1, \frac{dw_1}{dt}, w_2)$; (**f**) the phase portraits in the three-dimensional space $(\frac{dw_1}{dt}, w_2, \frac{dw_2}{dt})$.

According to the aforementioned analysis, the excitation coefficient and damping coefficient parameters play an important role on chaos of the sandwich plate with truss core. So we select the excitation coefficients f and damping coefficients μ as the controlling parameters to detect the chaotic dynamics for the sandwich plate. Figure 3 demonstrates the existence of the multi-pulse jumping chaotic motion when $\mu = 0.1$, $f = 50$. Do not change other parameters and initial conditions. The maximal Lyapunov exponent of system (12) is also calculated as 0.427282. It is easy to find that parameter conditions are also satisfied, which demonstrates the existence of the multi-pulse chaotic motion in Figure 3. Figure 4 represents the existence of the multi-pulse jumping chaotic motions when $\mu = 0.06$, $f = 100$. The maximal Lyapunov exponent of system (12) in this case is 0.450072. It is found that from Figure 4 that the phase portraits and waveforms are different from those given in Figures 2 and 3.This indicates that different μ and f have important impact on the chaotic motions of the sandwich plate with truss core. Finally, the Lyapunov exponent spectrum of system (12) for $f = 13.3$ and $f = 50$ are also given in Figure 5.

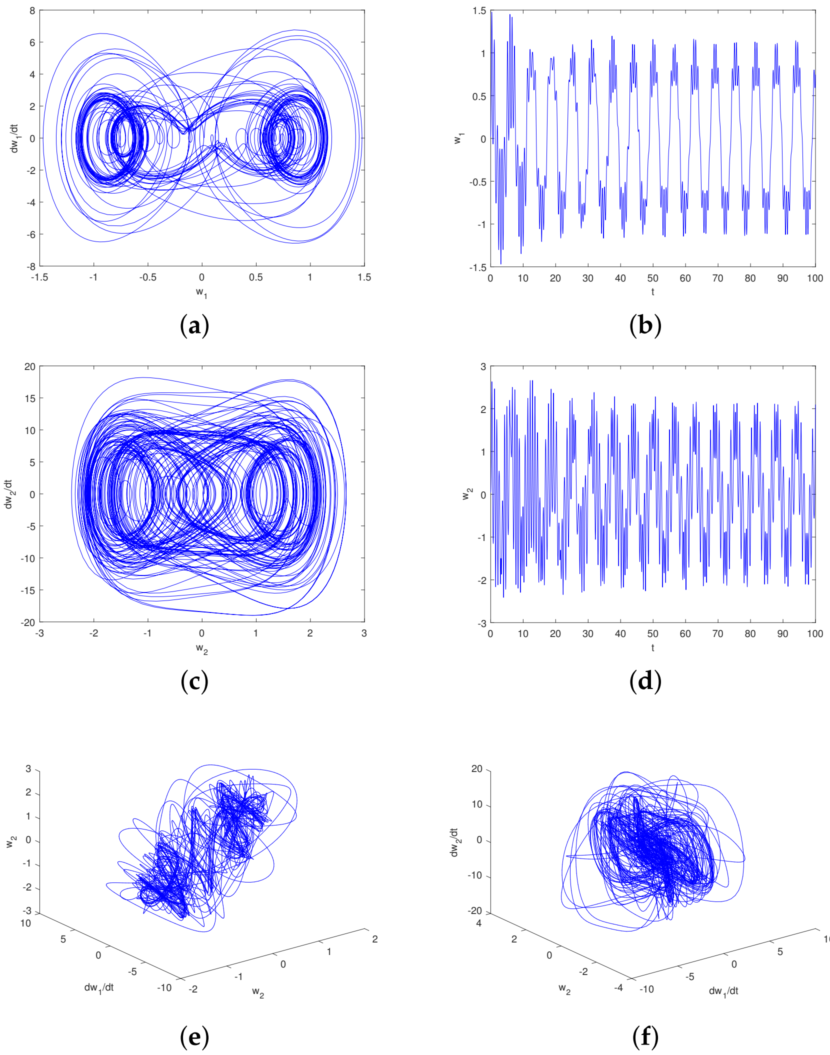

Figure 3. The phase portraits and waveforms of the sandwich plate with truss core when $\mu = 0.1$ and $f = 50$: (**a**) the phase portrait on plane $(w_1, \frac{dw_1}{dt})$; (**b**) the waveform on plane (t, w_1); (**c**) the phase portrait on plane $(w_2, \frac{dw_2}{dt})$; (**d**) the waveform on plane (t, w_2); (**e**) the phase portraits in the three-dimensional space $(w_1, \frac{dw_1}{dt}, w_2)$; (**f**) the phase portraits in the three-dimensional space $(\frac{dw_1}{dt}, w_2, \frac{dw_2}{dt})$.

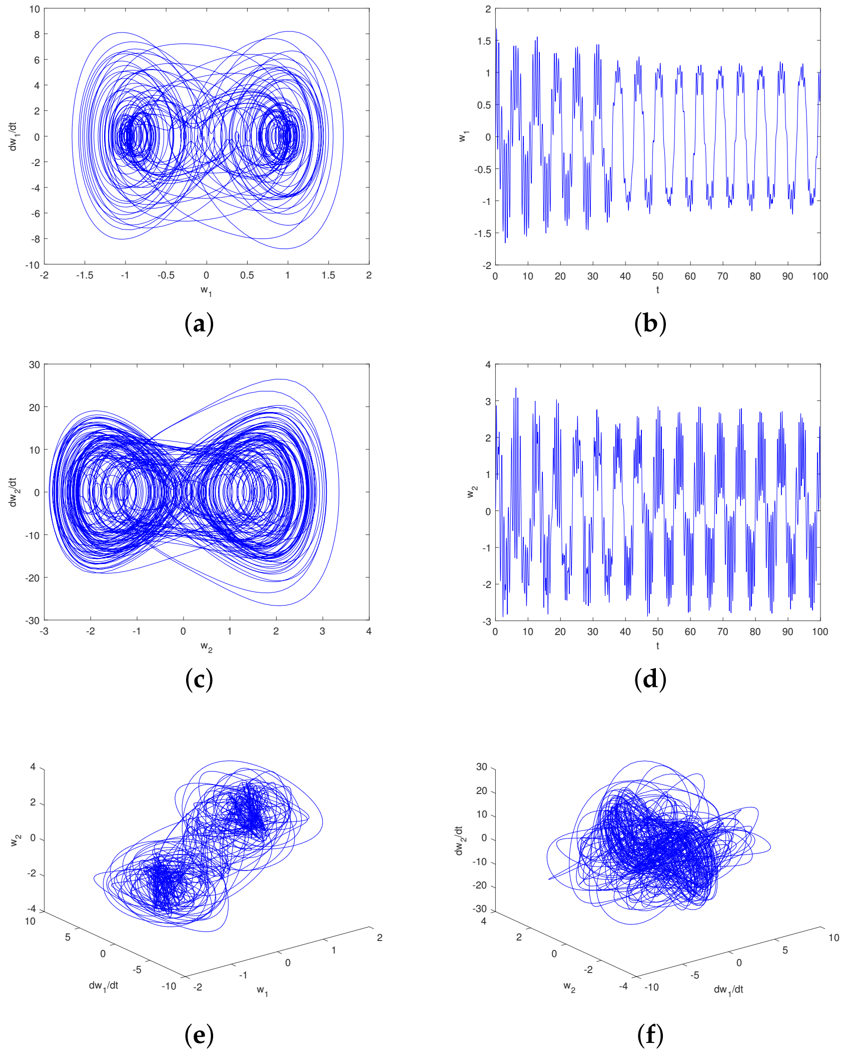

Figure 4. The phase portraits and waveforms of the sandwich plate with truss core when $\mu = 0.06$ and $f = 100$: (**a**) the phase portrait on plane $(w_1, \frac{dw_1}{dt})$; (**b**) the waveform on plane (t, w_1); (**c**) the phase portrait on plane $(w_2, \frac{dw_2}{dt})$; (**d**) the waveform on plane (t, w_2); (**e**) the phase portraits in the three-dimensional space $(w_1, \frac{dw_1}{dt}, w_2)$; (**f**) the phase portraits in the three-dimensional space $(\frac{dw_1}{dt}, w_2, \frac{dw_2}{dt})$.

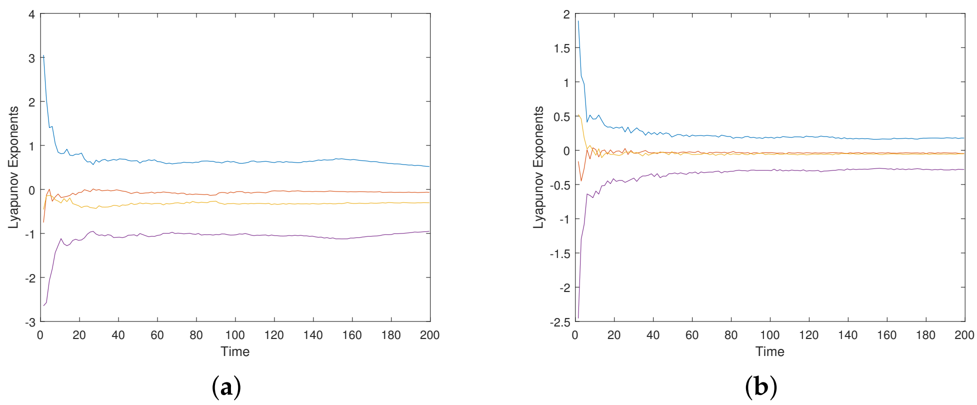

Figure 5. The Lyapunov exponent spectrum system (12): (**a**) when $\mu = 0.4$ and $f = 13.3$; (**b**) when $\mu = 0.1$ and $f = 50$.

5. Conclusions

The chaotic dynamics are investigated for a simply supported sandwich plate by using rigorous analytical approaches. The improved extended Melnikov method in [10,18] is applied to detect chaotic motions of the non-autonomous nonlinear system. By introducing Σ^{ϕ_0}, the four-dimensional non-autonomous system is transformed into a five-dimensional autonomous system, by which the chaotic motions can be investigated by directly employing this analytical method. The k-pulse Melnikov function M_k has simple zeros. Furthermore, we obtain the parameter conditions for the occurrence of chaotic motion.

Numerical simulations are also used to detect the complicated chaotic motions of the truss core sandwich plate model. Moreovecr, the numerical results verify the possibility of chaotic behaviors when the structural parameters satisfy specific conditions given by theoretical analysis. The chaotic motions of the sandwich plate with truss core can be exhibited by the phase portraits, the waveforms and the maximum Lyapunov exponents for different control parameters. Based on the theoretical analysis and numerical results, it is observed that the chaotic motions of the sandwich plate with truss core can be affected by the excitation coefficients and damping coefficients. Thus, the nonlinear dynamical behaviors of the sandwich plate model can be controlled by varying the structural damping and transverse excitations parameters, respectively. The analytic results bear certain guiding significance for the design and control of the system.

The extended Melnikov method is an effective theoretical technique in detecting the chaotic motions of the high-dimensional nonlinear system. However, a limitation of several analytical methods is that we must follow the special form of the high-dimensional system when detecting chaotic motions. Therefore, future work should focus on how to improve the analytical methods to adapt research of more general forms for a high-dimensional nonlinear system.

Author Contributions: D.Z.: Conceptualization, Data curation, Writing—original draft; F.L.: Methodology, Writing—review and editing. All authors have read and agreed to the published version of the manuscript.

Funding: This work is supported by the National Natural Science Foundation of China (Nos. 11902133 and 12071198).

Institutional Review Board Statement: Not applicable.

Informed Consent Statement: Not applicable.

Data Availability Statement: Not applicable.

Conflicts of Interest: The authors declare no conflict of interest.

References

1. Chen, J.E.; Liu, Y.Q.; Liu, W.; Su, X.Y. Themal buckling analysis of truss core sandwich plates. *Appl. Math. Mech.* **2013**, *34*, 1177–1186. [CrossRef]
2. Chen, J.E.; Zhang, W.; Yao, M.H.; Liu, J. Vibration reduction in truss core sandwich plate with internal nonlinear energy sink. *Compos. Struct.* **2018**, *193*, 180–188. [CrossRef]
3. Boorle, R.K.; Mallick, P.K. Global bending response of composite sandwich plates with coorugated core: Part I: Effect of geometric parameters. *Compos. Struct.* **2016**, *141*, 375–388. [CrossRef]
4. Zhang, W.; Chen, J.E.; Cao, D.X.; Chen, L.H. Nonlinear dynamic responses of a truss core sandwich plate. *Compos Struct.* **2014**, *108*, 367–386. [CrossRef]
5. Zhang, W.; Wu, Q.L.; Yao, M.H.; Dowell, E.H. Analysis on global and chaotic dynamics of nonlinear wave equations for truss core sandwich plate. *Compos. Struct.* **2018**, *94*, 21–37. [CrossRef]
6. Chen, Z.Y.; Chen, F.Q.; Zhou, L.Q. Slow-fast dynamics in the truss core sandwich plate under excitations with high and low frequencies. *Appl. Math. Model.* **2020**, *88*, 382–395. [CrossRef]
7. Li, F.; Jin, Y.L., Tian, Y. Integrability and linearizability of cubic Z2 systems with non-resonant singular points. *J. Diff. Equ.* **2020**, *269*, 9026–9049. [CrossRef]
8. Ramakrishnan, B.; Ahmadi, A.; Nazarimehr, F.; Natiq, H.; Jafari, S.; Hussain, I. Oyster oscillator: A novel mega-stable nonlinear chaotic system. *Eur. Phys. J. Spec. Top.* **2021** . [CrossRef]

9. Yao, M.H.; Zhang, W.; Yao, Z.G. Muti-pulse orbits dynamics of composite laminated piezoelectric rectangular plate. *Sci. China Technol. Sci.* **2011**, *154*, 2064–2079. [CrossRef]
10. Camassa, R.; Kovacic G.; Tin, S.K. A Melnikov method for homoclinic orbits with many pulse. *Arch. Ration Mech. Anal.* **1998**, *143*, 105–193. [CrossRef]
11. Yagasaki, K. The method of Melnikov for perturbations of multi-degree of freeedom Hamiltonian systems. *Nonlinearity* **1999**, *12*, 799–822. [CrossRef]
12. Yagasaki, K. Horseshoes in two-degree-of-freedom Hamiltonian systems with saddle-centers. *Arch. Rational Mech. Anal.* **2000**, *154*, 275–296. [CrossRef]
13. Yao, M.H.; Zhang, W.; Zu, J.W. Multi-pulse chaotic dynamics in non-planar motion of parametrically excited viscoelastic moving belt. *J. Sound Vib.* **2012**, *331*, 2624–2653. [CrossRef]
14. Zhang, W.; Zheng, Y.; Liu, T.; Guo, X.Y. Multi-pulse jumping double-parameter chaotic dynamics of eccentric rotating ring truss antenna under combined parametric and external excitations. *Nonlinear Dyn.* **2019**, *98*, 761–800. [CrossRef]
15. Zhang, D.M.; Chen, F.Q. Global bifurcations and single-pulse homoclinic orbits of a plate subjected to the transverse and in-plane excitations. *Math. Methods Appl. Sci.* **2017**, *40*, 4338–4339. [CrossRef]
16. Ahmadi, A.; Wang, X.; Fahimeh Nazarimehr, F.; Alsaadi, F.E.; Alsaadi, F.E.; Pham, V.T. Coexisting infinitely many attractors in a new chaotic system with a curve of equilibria: Its extreme multi-stability and Kolmogorov-Sinai entropy computation. *Adv. Mech. Eng.* **2019**, *2*, 1–8. [CrossRef]
17. Khalaf, A.J.M.; Abdolmohammadi, H.R.; Ahmadi, A.; Moysis, L.; Volos, C.; Hussain, I. Extreme multi-stability analysis of a novel 5D chaotic system with hidden attractors line equilibrium permutation entropy and its secure communication scheme. *Eur. Phys. J. Special Top.* **2020**, *229*, 1175–1188. [CrossRef]
18. Zhang, W.; Zhang, J.H.; Yao, M.H. The extended Melnikov method for non-autonomous nonlinear dynamical systems and application to multi-pulse chaotic dynamics of a buckled thin plate. *Nonlinear Anal. Real World Appl.* **2010**, *11*, 1442–1457. [CrossRef]
19. Zhang, J.H.; Zhang, W. Multi-pulse chaotic dynamics of non-autonomous nonlinear system for a honeycomb sandwich plate. *Acta Mech. Sin.* **2012**, *223*, 1047–1066. [CrossRef]
20. Wu, Q.L.; Zhang, W.; Dowell, E.H. Detecting multi-pulse chaotic dynamics of high-dimensional non-autonomous nonlinear system for circular mesh antenna. *Int. J. Non-Linear Mech.* **2018**, *102*, 25–40. [CrossRef]
21. Hao, W.L.; Zhang, W.; Yao, M.H. Multi-pulse chaotic dynamics of six-dimensional non-autonomous nonlinear system for a honeycomb sandwich plate. *Int. J. Bifurc. Chaos* **2014**, *24*, 1450138. [CrossRef]